



On the Use of Digital Image Correlation to Analyze the Mechanical Properties of Brittle Matrix Composites

François Hild, Jean-Noël Périé, Jacques Lamon, Matthieu Puyo-Pain

► To cite this version:

François Hild, Jean-Noël Périé, Jacques Lamon, Matthieu Puyo-Pain. On the Use of Digital Image Correlation to Analyze the Mechanical Properties of Brittle Matrix Composites. 2005, 14 p. hal-00013814

HAL Id: hal-00013814

<https://hal.science/hal-00013814v1>

Submitted on 17 Nov 2005

HAL is a multi-disciplinary open access archive for the deposit and dissemination of scientific research documents, whether they are published or not. The documents may come from teaching and research institutions in France or abroad, or from public or private research centers.

L'archive ouverte pluridisciplinaire **HAL**, est destinée au dépôt et à la diffusion de documents scientifiques de niveau recherche, publiés ou non, émanant des établissements d'enseignement et de recherche français ou étrangers, des laboratoires publics ou privés.

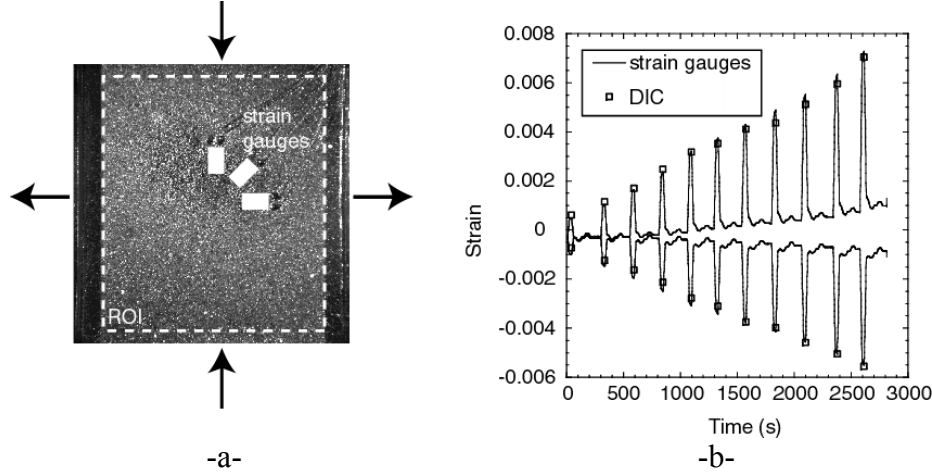


Figure 10. (a) Shear experiment, (b) comparison between gauge response and measurements by a digital image correlation technique ($l = 64$ pixels and $\delta = 32$ pixels).

Figure 11a shows the displacement field on the surface of the specimen just before the failure of the specimen. One can note the good symmetry of the displacement field about the two loading directions. The strain maps (Figs. 11b-c) show heterogeneities, which is a first indication that the material is not homogeneous on the scale of the measurements (of the order of 2-3 mm). It is worth remembering that the uncertainties related to the correlation technique are negligible for strain levels greater than 10^{-3} . Therefore, it can be stated that the strain field fluctuations are mainly due to material imperfections.

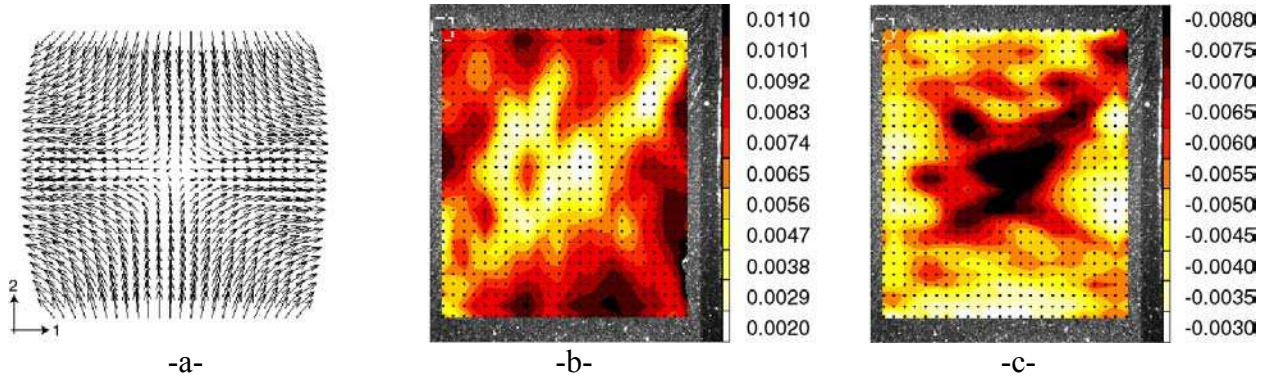


Figure 11. (a) Displacement field prior to failure (a). An amplification factor of 34 is used for the in-plane displacement vectors. Corresponding strain maps ϵ_{11} and ϵ_{22} .

To analyze the experimental results, one uses all the experimental points within the ROI (i.e., all the centers of the ZOIs, Fig. 11a). The strain field is directly deduced from the measured displacement field by a numerical derivation (e.g., Figs. 11b-c). As mentioned earlier, the damage fields can be used to predict the onset of failure related to the degradations in both plies. The damage field inside each layer within the ROI is obtained by a computation using a damage post-processor.³⁰ Figure 12 shows shear damage fields (d_{12}) in the $+45^\circ$ and -45° plies. As anticipated by the *a priori* computations (Fig. 9), shear damage increases more in the central part

of the specimen than near the edges. The damage field is heterogeneous and indicates a high degradation of the matrix, even more important (i.e., 0.6) than that observed in a tensile test at $\pm 45^\circ$ (i.e., 0.5³⁰). However, this damage field does not correspond to the actual failure pattern (Fig. 13c). Matrix damage is probably not the prevalent mechanism leading to the final failure of the specimen.

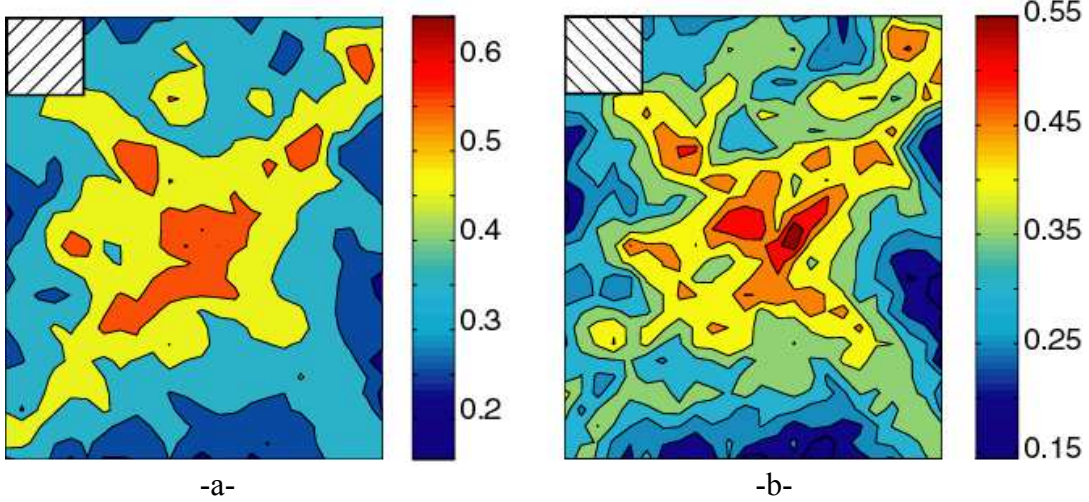


Figure 12. Matrix damage contours d_{12} in both ply directions predicted by a damage post-processor using strains deduced from full-field displacement measurements.

To predict failure, the relevant variable to consider is damage of the fibers (d_1), i.e., fiber breakage is likely to be the mechanism responsible for the final failure. Figures 13a-b show the damage field for the two ply orientations. The analysis of the damage contours in both ply directions can reproduce the overall failure pattern. This failure pattern is induced by the anisotropy of the material, and fiber breakage caused by the heterogeneity of the material on the scale of the measurements.

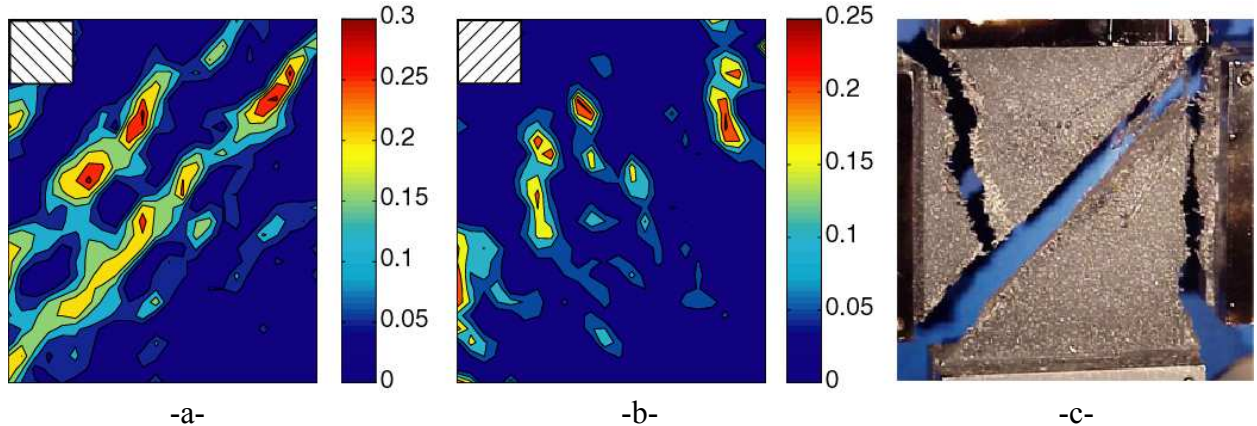


Figure 13. Fiber damage contours d_1 in both ply directions (a-b) predicted by a damage post-processor using strains deduced from a full-field displacement measurement and the final failure pattern (c).

These results show that a damage meso-model is able to capture the overall failure pattern (i.e., damage maps in both ply directions) and to conclude that fibers in both directions are damaged at the inception of a macrocrack. It is also important to note that these conclusions can be drawn only thanks to a full-field strain measurement (on the macro scale) used as input to a post-processor to evaluate the damage variables on the ply level (i.e., on the meso scale). Therefore, this test could be analyzed and a damage scenario could be proposed by combining full-field kinematic measurements and a damage model identified earlier.

SUMMARY

Digital image correlation is a well-suited technique for mechanical investigations dealing with brittle materials such as ceramics and ceramic-matrix composites. In particular, no special preparation of the surface is needed except for some applications that require a coating by a random black and white pattern. From experimental comparisons with conventional gauges, the strain uncertainty of the technique is shown to be equal to 2×10^{-4} when few measurement points are considered with an 8-bit CCD camera and can decrease to levels of the order of 10^{-5} or even 10^{-6} in favorable conditions with a 12-bit CCD camera for a larger gauge zone.

Two applications have been considered in the present paper. In a first study, local analyses were performed to determine elastic constants of a silicon-based joint. The DIC method allowed for accurate estimates of longitudinal displacements and strain fields even in extreme conditions, namely, low displacement and strain levels, high digital image magnification. The BraSiC elastic properties could be estimated and are comparable with those evaluated by a nanoindentation technique.

The second analysis deals with interactions between experimental data obtained on a C/C composite and mechanical investigations (here a shear experiment on a plate). The entire displacement field is considered to derive the strain field. A damage post-processor is applied to the experimental results to evaluate different damage fields describing matrix and fiber degradations. It is shown that fiber breakage causes the failure even when the overall load pattern is shear at $\pm 45^\circ$.

REFERENCES

- ¹P.K. Rastogi (ed.) "Photomechanics," Springer, Berlin (Germany), (2000).
- ²S. Calloch, F. Hild, C. Doudard, C. Bouvet, and C. L'Excellent, "Analyse d'essais de compression biaxiale sur un A.M.F. à l'aide d'une technique d'intercorrélation d'images numériques," in Proc. Photomécanique 2001, 207-214 (2001).
- ³C. G'Sell, J.-M. Hiver, A. Dahnoun, and A. Souahi, "Video-Controlled Tensile Testing of Polymers and Metals Beyond the Necking Point," *J. Mat. Sci.*, **27**, 5031-5039 (1992).
- ⁴X. Fayolle, "Corimage : programme de pilotage d'essais asservis sur une jauge de déformation optique," CNAM dissertation, CNAM Paris, (2004).
- ⁵J.N. Périé, S. Calloch, C. Cluzel, and F. Hild, "Analysis of a Multiaxial Test on a C/C Composite by Using Digital Image Correlation and a Damage Model," *Exp. Mech.*, **42**, 318-328 (2002).

⁶F. Hild, B. Raka, M. Baudequin, S. Roux, and F. Cantelaube, "Multi-Scale Displacement Field Measurements of Compressed Mineral Wool Samples by Digital Image Correlation," *Appl. Optics*, **IP 41**, 6815-6828 (2002).

⁷M. Bonnet, and A. Constantinescu, "Inverse problems in elasticity," *Inverse Problems*, **21**, R1-R50 (2005).

⁸W.H. Peters, and W.F. Ranson, "Digital imaging techniques in experimental stress analysis," *Opt. Eng.*, **21**, 427-431 (1982).

⁹M.A. Sutton, W.J. Wolters, W.H. Peters, W.F. Ranson, and S.R. McNeill, "Determination of Displacements Using an Improved Digital Correlation Method," *Im. Vis. Comp.*, **1**, 133-139 (1983).

¹⁰Z. Sun, J.S. Lyons, and S.R. McNeill, "Measuring microscopic deformations with digital image correlation," *Opt. Lasers Eng.*, **27**, 409-428 (1997).

¹¹W.G. Knauss, I. Chasiotis, and Y. Huang, "Mechanical measurement at the micron and nanometer scales," *Mech. Mat.*, **35**, 217-231 (2003).

¹²P. Forquin, L. Rota, Y. Charles, and F. Hild, "A Method to Determine the Toughness Scatter of Brittle Materials," *Int. J. Fract.*, **125**, 171-187 (2004).

¹³T.C. Chu, W.F. Ranson, M.A. Sutton, and W.H. Petters, "Applications of Digital-Image-Correlation Techniques to Experimental Mechanics," *Exp. Mech.*, **3**, 232-244 (1985).

¹⁴D.J. Chen, F.P. Chiang, Y.S. Tan, and H.S. Don, "Digital Speckle-Displacement Measurement Using a Complex Spectrum Method," *Appl. Opt.*, **32**, 1839-1849 (1993).

¹⁵Y. Berthaud, J. Scholz, and J. Thesing, "Méthodes optiques et acoustiques de mesures des caractéristiques mécaniques," in Proc. *Colloque national MECAMAT "Mécanismes et mécanique des grandes déformations"*, 77-80 (1996).

¹⁶F.P. Chiang, Q. Wang, and F. Lehman, "New Developments in Full-Field Strain Measurements Using Speckles," in *Non-Traditional Methods of Sensing Stress, Strain and Damage in Materials and Structures*, 156-169, ASTM, Philadelphia (USA), (1997).

¹⁷R.W. Messler Jr, "Joining of advanced materials," Butterworth-Heinemann, Boston (USA), (1993).

¹⁸M.M. Schwartz, "Ceramic joining," American Society for Metals, Materials Park (USA), (1990).

¹⁹M.G. Nichols, "Joining of ceramics," Chapman & Hall, London (UK), (1990).

²⁰C.H. Bates, M.R. Foley, G.A. Rossi, G.J. Sundberg, and F.J. Wu, "Joining of non-oxide ceramics for high-temperature applications," *Am. Ceram. Soc. Bull.*, **69**, 350-356 (1990).

²¹O.M. Akselsen, "Advances in brazing of ceramics," *J. Mat. Sci.*, **27**, 1989-2000 (1992).

²²M.R. Locatelli, B.J. Dagleish, K. Nakashima, A.P. Tomsia, and A.M. Glaeser, "New approaches to joining ceramics for high-temperature applications," *Ceram. Intern.*, **23**, 313-322 (1997).

²³M. Singh, "Joining of sintered silicon carbide ceramics for high-temperature applications," *J. Mat. Sci. Letters*, **17**, 459-461 (1998).

²⁴A. Gasse, "Rôle des interfaces dans le brasage non réactif du SiC par des siliciures de Co et de Cu," *PhD dissertation (in French)*, INPG, (1996).

²⁵F. Moret, P. Sire, and A. Gasse, "Brazing of SiC based materials using the BraSiC process chemical and thermal applications," in Proc. *International Conference on Joining of Advanced Materials* (1998).

²⁶J. Martinez Fernandez, A. Munoz, F.M. Varela-Feria, and M. Singh, "Interfacial and thermomechanical characterization of reaction formed joints in silicon carbide-based materials," *J. Eur. Ceram. Soc.*, **20**, 2641-2648 (2000).

²⁷C.A. Lewinsohn, H. Serizawa, and H. Murakawa, "FEM analysis of experimental measurement technique for mechanical strength of ceramic joints," in Proc. *Ceramic Engineering and Science Proceedings*, **22**, 635-642 (2001).

²⁸M. Singh, and E. Lara-Curzio, "Design, fabrication, and testing of ceramic joints for high temperature SiC/SiC composites," *J. Eng. Gas Turb. Power*, **123**, 288-292 (2001).

²⁹M. Puyo-Pain, "Comportement mécanique d'assemblages de composites 2D SiC/SiC brasés par un joint à base de silicium : mesures de champs par corrélation d'images numériques en conditions extrêmes," *PhD dissertation (in French)*, University of Bordeaux 1, no. 2905, (2004).

³⁰J.-N. Périé, "Méso-modélisation des mécanismes d'endommagement dans les composites C/C à texture multidirectionnelle," *Ph.D. dissertation*, ENS de Cachan, (2000).

³¹J.-N. Périé, X. Aubard, C. Cluzel, and P. Ladevèze, "Méso-modélisation des mécanismes d'endommagement d'une famille de matériaux Sepcarb® à textures multidirectionnelles," in Proc. *JNC11*, 883-888 (1998).

³²P. Ladevèze, "On an anisotropic damage theory," in Proc. *CNRS International Colloquium no. 351 'Failure criteria of structured media'*, 355-365 (1983).